Cell Reports
Article

ER Stress Causes Rapid Loss of Intestinal Epithelial Stemness through Activation of the Unfolded Protein Response

Jarom Heijmans,[1] Jooske F. van Lidth de Jeude,[1] Bon-Kyoung Koo,[4] Sanne L. Rosekrans,[1] Mattheus C.B. Wielenga,[1] Marc van de Wetering,[4] Marc Ferrante,[4] Amy S. Lee,[5] Jos J.M. Onderwater,[3] James C. Paton,[6] Adrienne W. Paton,[6] A. Mieke Mommaas,[3] Liudmila L. Kodach,[2] James C. Hardwick,[2] Daniël W. Hommes,[2,7] Hans Clevers,[4] Vanesa Muncan,[1] and Gijs R. van den Brink[1,*]

[1]Tytgat Institute for Liver and Intestinal Research and Department of Gastroenterology and Hepatology, Academic Medical Center, 1105 AZ Amsterdam, the Netherlands
[2]Department of Gastroenterology and Hepatology
[3]Electron Microscopy Section, Department of Molecular Cell Biology
Leiden University Medical Center, 2333 ZA Leiden, the Netherlands
[4]Hubrecht Institute, 3584 CT Utrecht, the Netherlands
[5]Department of Biochemistry and Molecular Biology, USC/Norris Comprehensive Cancer Center, University of Southern California Keck School of Medicine, Los Angeles, CA 90033, USA
[6]Research Centre for Infectious Diseases, School of Molecular and Biomedical Science, University of Adelaide, South Australia 5005, Australia
[7]Center for Inflammatory Bowel Diseases, University of California, Los Angeles, CA 90095, USA
*Correspondence: g.r.vandenbrink@amc.nl
http://dx.doi.org/10.1016/j.celrep.2013.02.031

SUMMARY

Stem cells generate rapidly dividing transit-amplifying cells that have lost the capacity for self-renewal but cycle for a number of times until they exit the cell cycle and undergo terminal differentiation. We know very little of the type of signals that trigger the earliest steps of stem cell differentiation and mediate a stem cell to transit-amplifying cell transition. We show that in normal intestinal epithelium, endoplasmic reticulum (ER) stress and activity of the unfolded protein response (UPR) are induced at the transition from stem cell to transit-amplifying cell. Induction of ER stress causes loss of stemness in a Perk-eIF2α-dependent manner. Inhibition of Perk-eIF2α signaling results in stem cell accumulation in organoid culture of primary intestinal epithelium. Our findings show that the UPR plays an important role in the regulation of intestinal epithelial stem cell differentiation.

INTRODUCTION

Intestinal stem cells or so-called crypt base columnar (CBC) cells are morphologically recognizable as slender columnar cells that lie interspersed with Paneth cells at the base of the crypt and express stem cell markers such as *Lgr5*, *Olfm4*, and *Ascl2* (Barker et al., 2007; van der Flier et al., 2009). Stem cells divide and form transit-amplifying (TA) cells, which are localized higher up in the crypts just above the level of the uppermost Paneth cell. TA cells cycle a number of times and differentiate into the different epithelial lineages of the small intestine.

During cellular differentiation, a broad range of specialized transmembrane and secreted proteins is produced that requires processing in the endoplasmic reticulum (ER). The accumulation of nascent proteins in the ER attract chaperones such as Grp78, that are normally bound to the ER membrane (Ni and Lee, 2007). This shifts Grp78 away from binding to three distinct transmembrane receptors, Ire1α, Atf6, and Perk (Harding et al., 2002) and is one of the mechanisms through which these receptors activate an ER stress response called the unfolded protein response (UPR). Ire1α activates transcription factor Xbp1, and Atf6 is cleaved to generate a transcriptionally active fragment. The resulting transcriptional response increases the capacity of the ER. The PKR-like ER kinase (Perk) phosphorylates the translation initiation factor eIF2α and thereby causes temporary translation attenuation. Altogether, UPR signals from the ER are critical to resolve ER stress and restore homeostasis in the ER. Or, if ER stress remains unresolved, apoptosis is induced (Harding et al., 2002).

In the intestine, the UPR transcription factor Xbp1 is involved in the maintenance of secretory cell lineages and has been associated with the risk of developing inflammatory bowel disease (Kaser et al., 2008). However, the role of ER stress and UPR signaling in the intestinal epithelium remains incompletely understood. Here, we use a combination of genetic and cellular techniques to characterize their function. Our data reveal a role for ER stress and Perk-eIF2α signaling in mediating differentiation of intestinal epithelial stem cells.

RESULTS

ER Stress Is Low in Intestinal Stem Cells Compared to TA Cells

To localize the occurrence of ER stress and UPR signaling in the normal intestine, we examined the expression of components

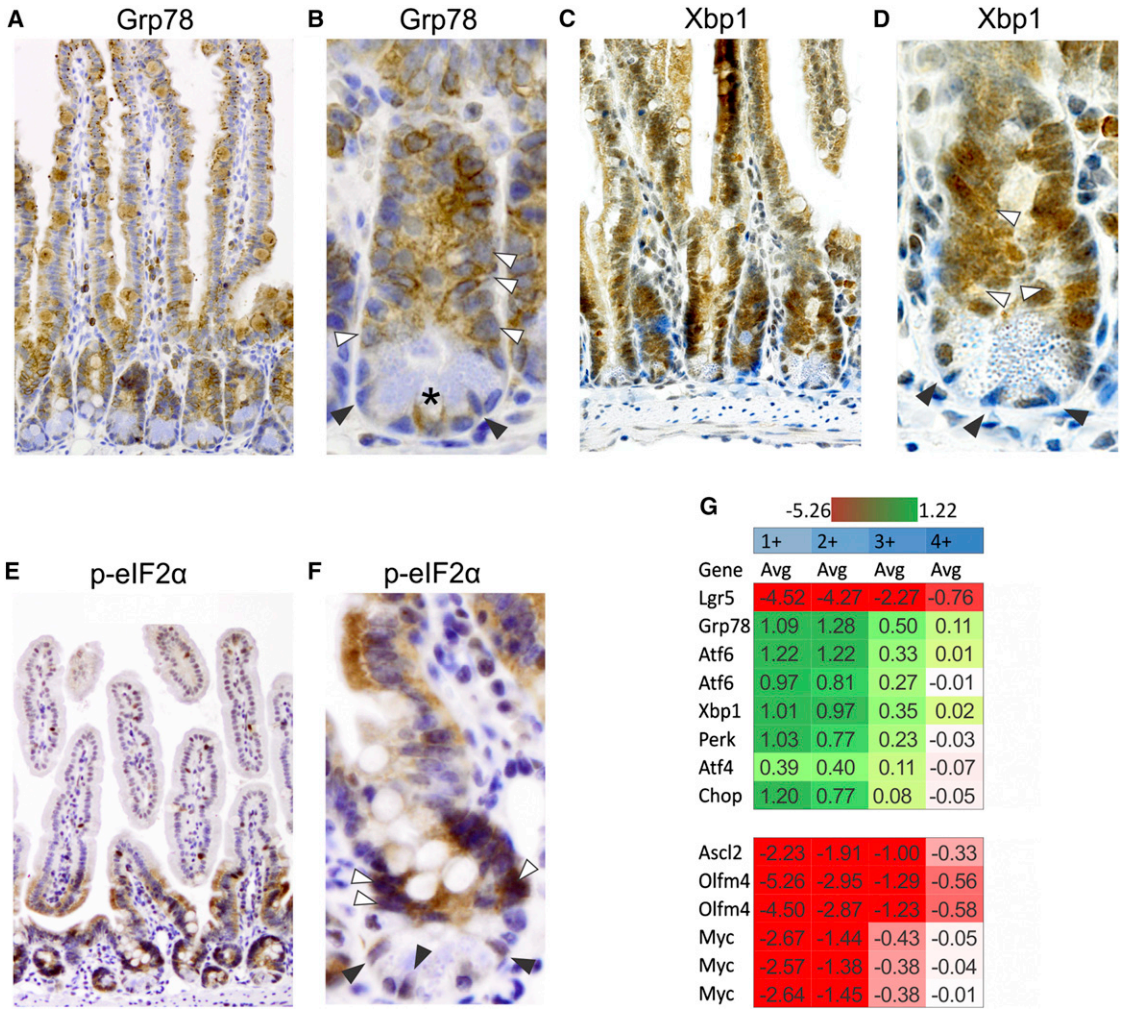

Figure 1. Components of the UPR Are Expressed from the Level of Transit-Amplifying Cells Upward

(A–F) Immunohistochemistry (A and B) expression of Grp78. Black arrowheads point at crypt base columnar (CBC) cells at the stem cell position, white arrowheads point to TA cells, and dashed lines delineate crypts. The asterisk in (B) marks a single high-expressing Paneth cell. (C and D) IHC for Xbp1; activity of Xbp1 can be seen by nuclear localization of the protein that is high in TA cells (white arrowheads) compared to CBC stem cells (black arrowheads). (E and F) Phospho-specific detection of eIF2α shows a similar differential expression between TA cells (white arrowheads) and CBC stem cells (black arrowheads).

(G) Two log fold change values of indicated genes in sorted cell populations normalized to their expression in population +5 (*Lgr5*^{hi} cells). Expression gradients of markers of stemness and the activity of the UPR are inversely correlated. Each row depicts one probe on the microarray.

Original magnifications: 200× in (A), (C), and (E); 400× in (B), (D), and (F).

See also Figure S1.

and targets of the UPR. The chaperone Grp78 acts as a repressor of the UPR (Bertolotti et al., 2000) and is one of its major transcriptional targets and therefore widely used as readout for ER stress signaling (Mao et al., 2004). Analysis by immunohistochemistry (IHC) showed that Grp78 expression was low in the stem cells and high in the TA cells higher up in the crypt and in differentiated cells on the villus (Figures 1A and 1B). Expression of components and targets of the three arms of the UPR followed a similar pattern. Levels of both Xbp1 (Figures 1C and 1D) and phospho-eIF2α (Figures 1E and 1F) were very low in crypt base columnar cells compared to TA cells higher up in the crypt. It was previously shown that differentiation of Paneth cells depends on UPR signaling (Kaser et al., 2008). We found that expression of UPR components was heterogeneous in these cells with only a subset of Paneth cells expressing high levels of Grp78, Xbp1, and phospho-eIF2α (Figure S1 available online). This suggests that activation of the UPR may regulate a specific stage of Paneth cell differentiation or activation. To confirm the difference in levels of ER stress and UPR signaling between stem cells and TA cells, we analyzed markers of ER stress in gene arrays performed on sorted intestinal epithelial stem cells (Muñoz et al., 2012). In this experiment, we used the intestinal epithelium of *Lgr5-eGFP* mice, sorted in five different populations of cells based on the intensity of eGFP expression. We marked the highest expressing population as +5 and the lowest eGFP expressors as +1. Differential analysis of these

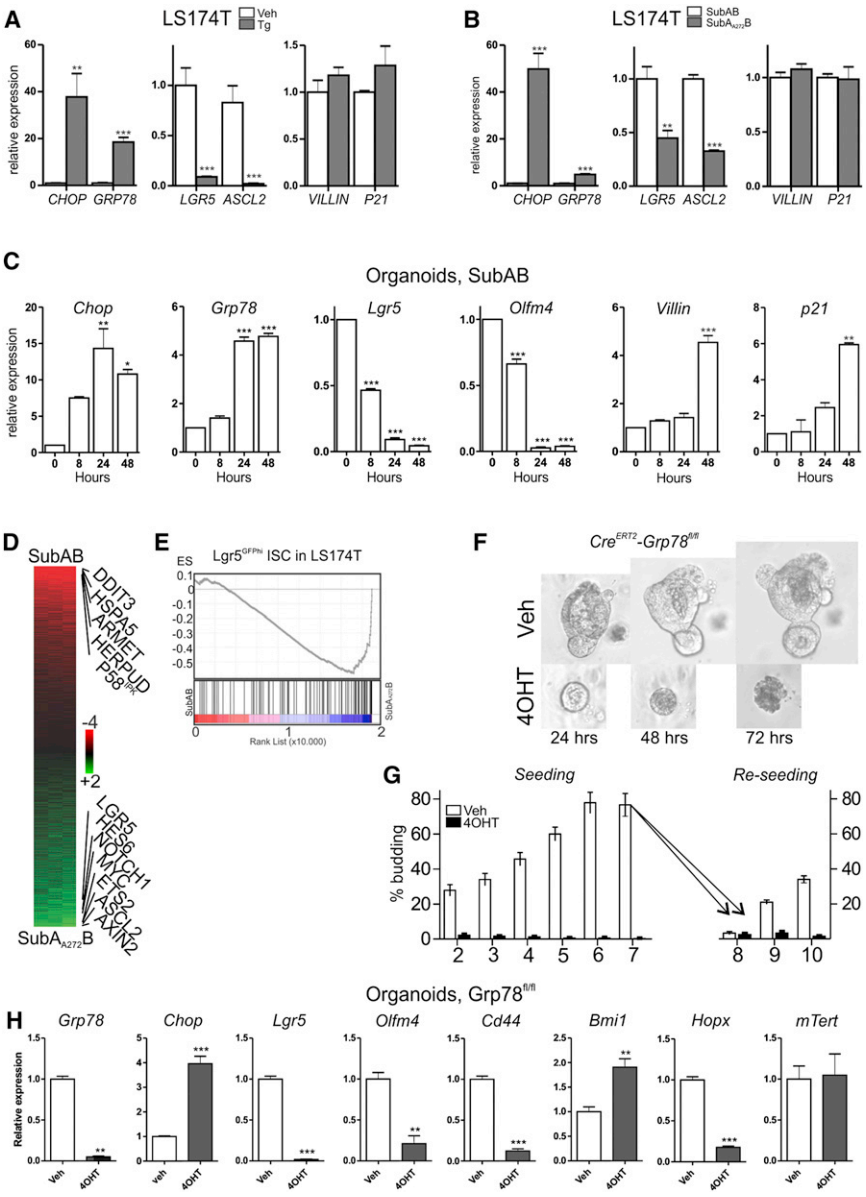

Figure 2. ER Stress Reduces Expression of Markers of Intestinal Epithelial Stemness In Vitro

(A and B) Quantitative RT-PCR for UPR markers *CHOP* and *GRP78*, stem cell markers *LGR5* and *ASCL2*, and differentiation markers *VILLIN* and *P21* in LS174T cells treated for 24 hr with 200 nM thapsigargin versus vehicle or 100 ng/ml SubAB versus $SubA_{A272}B$.

(C) Quantitative RT-PCR for UPR markers *Chop* and *Grp78*, stem cell markers *Lgr5* and *Olfm4*, and differentiation markers *Villin* and *p21* in organoids at different time points after treatment with 100 ng/ml SubAB or protease-dead $SubA_{A272}B$.

(D) Gene expression analysis of SubAB-treated LS174T cells results in loss of several stem cell markers and upregulation of UPR target genes.

(E) GSEA of $Lgr5^{hi}$ genes in LS174T cells after treatment with SubAB shows profound loss of the stemness signature.

(F) Bright-field images of $Grp78^{fl/fl}$ organoids that were treated with either vehicle or 4OHT shows reduced growth in organoids that lack Grp78.

(G) Quantification of *CreERT2-Grp78*$^{fl/fl}$ organoids after treatment with vehicle or 4-OH tamoxifen (4OHT). Seven days after treatment, non-recombined organoids were harvested, reseeded, and treated with either vehicle or 4OHT, showing growth inhibition of organoids that lack Grp78.

(H) Quantitative RT-PCR for UPR markers and a panel of stem cell markers on *CreERT2-Grp78*$^{fl/fl}$ organoids shows robust loss markers of crypt base columnar stem cell, but not alternatively proposed stem cell markers *Bmi1* and *mTert*.

Tg, thapsigargin. Values in (A)–(C), (G), and (H) are mean ± SEM, $^{**}p < 0.01$, $^{***}p < 0.001$.

See also Figure S2.

cell populations showed that stem cell markers *Lgr5*, *Ascl2*, and *Olfm4* were strongly enriched in the eGFP +5 population compared to the +1 population as expected. Markers of ER stress and components of the UPR clearly showed an inverse correlation with markers of stemness (Figure 1G). Taken together, these results suggest that stem cells are low in ER stress and that activation of the UPR occurs in TA cells and differentiated cells.

Induction of ER Stress Causes Loss of the Stem Cell Signature In Vitro

Since we observed a differential activity of the UPR between stem cells and TA cells, we examined the consequence of increased ER stress on intestinal epithelial stemness. For in vitro experiments, we used the LS174T colon cancer cell line, since its transcriptional profile resembles that of stem cells and TA cells (van de Wetering et al., 2002). These cells have been successfully used in the initial screens that have identified intestinal epithelial stem cell markers such as *Lgr5* and *Ascl2* (Barker et al., 2007; Van der Flier et al., 2007, 2009). To induce ER stress in LS174T cells, we treated them with thapsigargin. This resulted in upregulation of targets of the UPR such as *CHOP* and *GRP78* as expected (Figure 2A). Treatment with thapsigargin resulted in marked repression of stem cell markers *LGR5* and *ASCL2*, whereas the expression of differentiation markers *VILLIN1* and *P21* was not affected (Figure 2A). To confirm this pharmacological approach, we used subtilase cytotoxin (SubAB) to deplete cells of GRP78. This bacterial toxin specifically inactivates GRP78 inside the ER by proteolysis (Paton et al., 2006). Apart from being a target of the UPR, GRP78 serves as an important repressor of the UPR and as an ER-localized chaperone (Bertolotti et al., 2000; Pfaffenbach and Lee, 2011). Similar to treatment with thapsigargin, SubAB-mediated GRP78 depletion resulted in cell-cycle arrest (data not shown) and upregulation of targets of the UPR and reduction

of expression of both *LGR5* and *ASCL2*, whereas expression of *VILLIN1* and *P21* was not affected (Figure 2B). LS174T cells express the intestinal epithelial stemness signature, but these cells are colorectal cancer cells. We therefore used cultured organoids of primary intestinal epithelium (Sato et al., 2009) to confirm the effect of activation of the UPR on stem cell markers in untransformed cells. Organoids have crypt and villus domains, contain normal numbers of stem cells per crypt, and serve as a useful model for the study of cellular differentiation. We treated organoids with SubAB, which activated the UPR and resulted in rapid and near-complete loss of expression of stem cell markers *Lgr5* and *Olfm4* (Figure 2C). Loss of these stem cell markers was already apparent at 8 hr of treatment. Despite the loss of expression of stem cell markers at 24 hr, organoids still looked morphologically normal (Figure S2A). In the next 24 hr, crypts were slowly lost from the organoids, whereas the central villus domain was maintained (Figure S2A). At 48 hr of SubAB treatment, we observed upregulation of both *Villin1* and *p21* expression, suggesting increased enterocyte differentiation (Figure 2C). We performed microarray analysis of LS174T cells after treatment with SubAB or protease-dead $SubA_{A272}B$ (Figure 2D) and analyzed differentially expressed genes by gene ontology analysis. The most significantly activated pathways were ER overload response, endoplasmic reticulum, and UPR ($p = 2.9E10^{-20}$, $p = 2.4E10^{-16}$, $p = 4.4E10^{-13}$, respectively). The pathways DNA replication, DNA strand elongation, and cell cycle were among the most significantly downregulated pathways ($p = 6.0E10^{-12}$, $p = 3.4E^{-11}$, $p = 2.5E10^{-11}$, respectively). Thus, depletion of Grp78 can serve as a bona fide model to study ER stress signaling. We further analyzed a set of intestinal stem cell markers in our data set. For this, we used the published list of genes that are high in stem cells isolated from *Lgr5-eGFP* mice (van der Flier et al., 2009). Gene set enrichment analysis (GSEA) revealed that induction of ER stress causes profound de-enrichment of these intestinal epithelial stem cell markers (normalized enrichment score −2.013, nominal p value < 0.001, false discovery rate [FDR] q value < 0.001) (Figure 2E). This suggests that ER stress signaling reduces intestinal epithelial stemness.

We next assessed whether cells that experience ER stress still possessed the capacity for self-renewal. To this end, we generated organoids from mice that homozygously carry the conditional allele for *Grp78* (Luo et al., 2006). To enable inducible deletion of Grp78, we transduced these organoids with a retrovirus carrying tamoxifen-sensitive Cre recombinase (*CreERT2*). In these organoids, Grp78 can be deleted by treatment with 4-OH tamoxifen (4OHT). We confirmed successful recombination using this approach in $Rosa26^{zsGreen}$ reporter organoids (Figure S2B). We seeded *CreERT2-Grp*$^{fl/fl}$ organoids and treated them with 4OHT or vehicle. Whereas vehicle-treated organoids exhibited normal expansion of the number of crypts per organoid, 4OHT-treated organoids retained their initial size for a number of days and then regressed with cells dying off (Figure 2F). When 4OHT-treated *CreERT2-Grp78*$^{fl/fl}$ organoids were reseeded, they failed to establish new organoids (Figure 2G), indicating that the stem cells had lost their capacity for self-renewal. We next assessed whether loss of self-renewal capacity in *CreERT2-Grp78*$^{fl/fl}$ organoids is accompanied by loss of stem cells. We therefore treated these organoids with vehicle or 4OHT for 24 hr and harvested them for RNA expression studies 24 hr later. Genes that are highly expressed in crypt base columnar stem cells, such as *Lgr5*, *Olfm4*, and *Cd44*, were significantly downregulated upon deletion of Grp78. Interestingly, genes that mark alternatively proposed stem cell populations were upregulated (*Bmi1*), unaltered (*mTert*), or decreased (*Hopx*). Together, these data suggest that knockout of Grp78 causes loss of self-renewal capacity, accompanied by loss of crypt base columnar stem cells. Genes that mark alternative stem cell populations are not unequivocally altered.

Induction of ER Stress Results in Loss of Stem Cells In Vivo

To examine the effect of ER stress on intestinal epithelium in vivo, we generated mice in which we conditionally inactivated Grp78. We crossed mice harboring the *Grp78*-floxed allele to *Ah1Cre* mice (Ireland et al., 2004). In *Ah1Cre* mice, treatment with β-naphtoflavone induces expression of Cre in the crypts and lower part of the villus of the intestinal epithelium but not in Paneth cells (Ireland et al., 2004, 2005) (see also Figure S3A). Recombination in the long-lived stem cells that maintain small intestinal epithelium under homeostatic conditions is virtually 100% (Ireland et al., 2004) (see also Figure S3B). To monitor recombination, we used the $Rosa26^{LacZ}$ reporter allele (Soriano, 1999). Littermate *Ah1Cre-Grp78*$^{+/+}$ mice were used as controls. In the epithelium of *Ah1Cre-Grp78*$^{fl/fl}$, messenger RNA (mRNA) of targets of the UPR such as *Xbp1(s)* and *Chop* was upregulated at day 2 postinduction (p.i.) (Figure 3A). At day 1 p.i., IHC showed nuclear Xbp-1 and phosphorylated-eIF2α in the CBCs in Grp78 mutant animals (Figure S4). Additionally, the ER was expanded and appeared dilated in absorptive enterocytes of *Ah1Cre-Grp78*$^{fl/fl}$ mutant mice (data not shown). Recombination efficiency was high, with >99% $LacZ^+$ crypts at day 1 p.i. in both *Ah1Cre-Grp78*$^{fl/fl}$ and *Ah1Cre-Grp78*$^{+/+}$ animals (Figure 3B). In the first 2 days after induction, the intestine of *Ah1Cre-Grp78*$^{fl/fl}$ mice appeared grossly normal, but at day 3 p.i. crypts became hypoplastic with thinning of the epithelial layer. Over the next 2 days, an increasing amount of hyperplastic crypts evolved until the epithelium had regained an almost normal appearance on day 5 (Figure S5). We found that from day 3 onward, the epithelium showed increasing presence of LacZ-negative, Grp78-proficient (nonrecombined, wild-type) cells until almost the whole epithelium was repopulated by wild-type cells at day 5 p.i. (Figures 3B and 3C). These results show that despite low levels of expression, Grp78 serves a critical role in epithelial stem cells. It has previously been demonstrated that *Ah1Cre*-mediated deletion of genes that are pivotal for stem cell fate causes repopulation by wild-type cells that have escaped Cre-mediated recombination. Examples include *c-Myc* (Muncan et al., 2006) and the stem-cell-specific transcription factor *Ascl2* (van der Flier et al., 2009). To further investigate loss of self-renewal capacity of mutant epithelium, we analyzed the presence of stem cells by mRNA in situ hybridization for stem cell marker *Olfm4*. In *Ah1Cre-Grp*$^{fl/fl}$ mice, stem cells are already almost entirely lost at day 1 p.i. Between day 3 and 5 p.i., an increased number of $Olfm4^+$ stem-cell-containing crypts reappear (Figure 4A). A similar manner of repopulation was observed when we performed IHC for Grp78 (Figure 4B). Serial sections

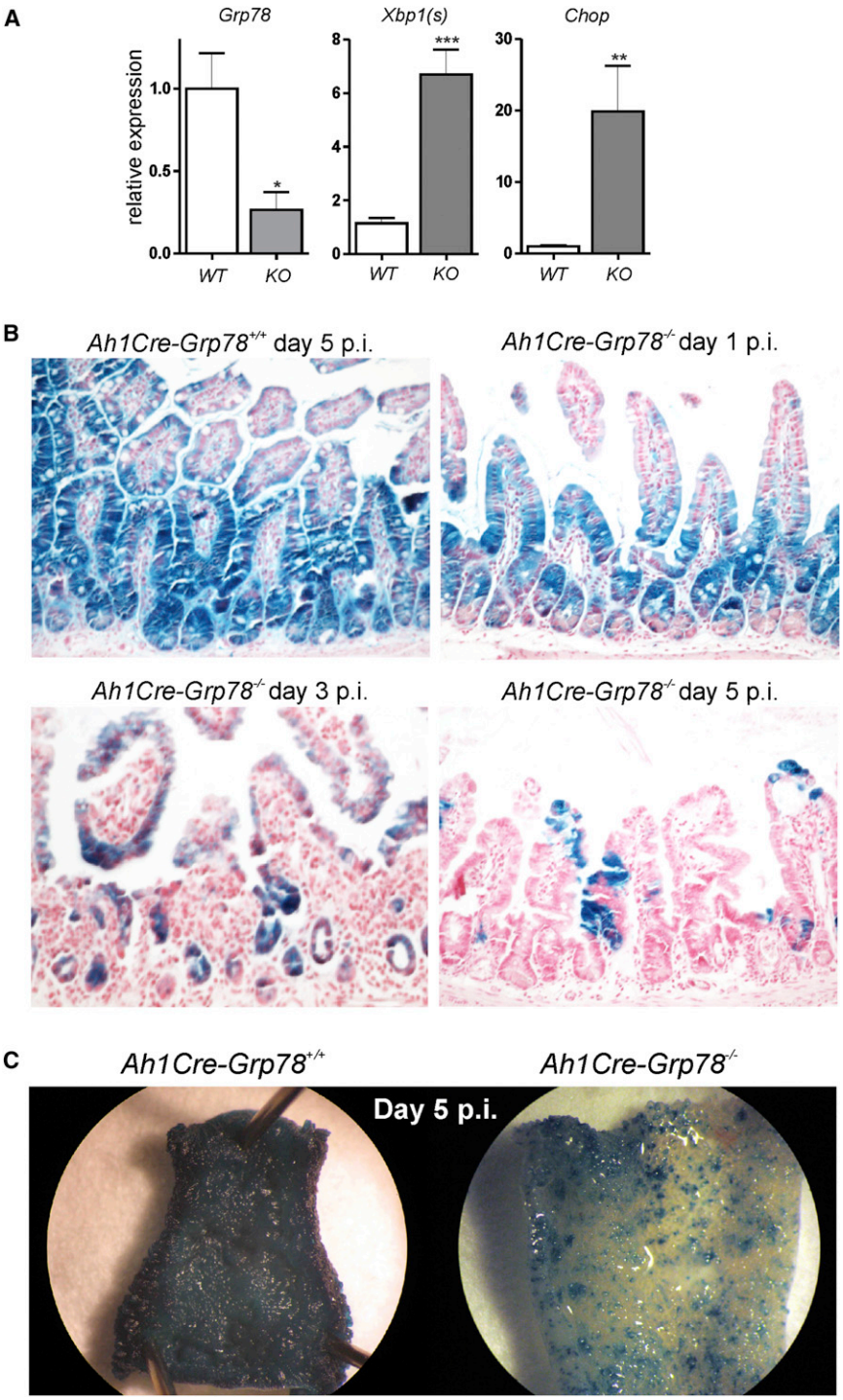

Figure 3. Rapid Repopulation by Unrecombined Cells upon Induction of ER Stress by Grp78 Deletion In Vivo

(A) Quantitative RT-PCR for the floxed exon of *Grp78* on epithelial scrapings of *AhCre1-Grp78*$^{fl/fl}$ and *AhCre1-Grp78*$^{+/+}$ control animals at day 2 p.i. (n = 3 per group) confirms loss of the targeted allele. UPR targets such as the spliced form of *Xbp1* (*Xbp1[s]*) and *Chop* are upregulated.

(B) LacZ staining on sections on day 1, 3, and 5 p.i. shows gradual repopulation of the epithelium of *AhCre1-Grp78*$^{fl/fl}$ mice by wild-type cells.

(C) Whole-mount LacZ staining shows almost complete repopulation in the mutant mouse at 5 days p.i.

Values in (A) are mean ± SEM, *p < 0.05, **p < 0.01, ***p < 0.001. WT, *AhCre1-Grp78*$^{+/+}$; KO, *AhCre1-Grp78*$^{fl/fl}$. Original magnifications in (B), 125×. See also Figures S3, S4, and S5.

localize these *Olfm4*$^{+}$ cells inside crypts that harbor Grp78-proficient (wild-type) cells (Figure 4C). Thus, induction of ER stress by deletion of Grp78 in the intestinal epithelium confirmed our in vitro experiments in which we found that ER stress leads to rapid loss of intestinal epithelial stemness.

Since unresolved ER stress can result in apoptosis, we examined if apoptosis could explain loss of stem cells. We observed a transient modest increase of active caspase-3 and TUNEL-positive cells in the crypts around 3 days p.i., 2 days after the loss of stem cells (Figure S6). Thus, low levels of apoptosis are induced upon loss of Grp78, possibly through unresolved ER stress. This was an unlikely cause for the rapid loss of expression stem cell markers we observed at day 1 p.i. To further characterize the effect of loss of Grp78 on crypt cells, we examined their proliferative potential at different time points after recombination. We found that incorporation of bromodeoxyuridine (BrdU) in Grp78 mutant crypts (as determined using consecutive sections stained for Grp78 and BrdU) remained normal at day 1 p.i. to extinguish only at day 3 p.i. (Figures 5A–5C and S5). This suggests that, although stem cells are rapidly lost, proliferation of TA cells is unaffected at first and that stem cells may have adopted a TA-cell-like phenotype.

Stressed Stem Cells Are Removed by Differentiation

We were unable to detect apoptosis in CBC cells at day 1 p.i. We therefore examined the *Grp78* mutant mice for an alternative cause of the disappearance of *Olfm4* expression and loss of self-renewal capacity of the mutant epithelium. We analyzed multiple crypt bases by electron microscopy at day 1 p.i. This revealed that, in mutant mice, CBC stem cells either had disappeared leaving adjacent Paneth cells or alternatively had increased width to height ratio and contained increased amounts of ER and mitochondria (Figures 5D–5G). These changes gave mutant CBC cells a TA-cell-like appearance.

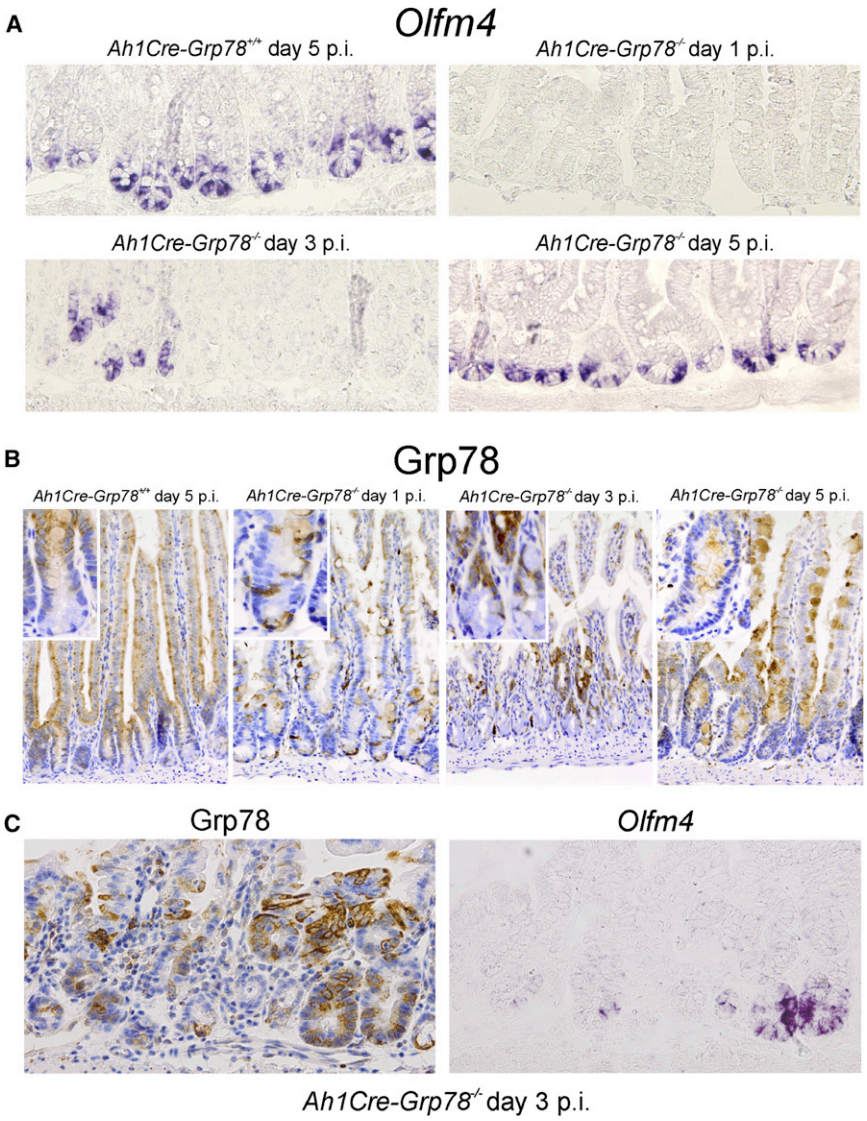

Figure 4. Repopulation of the Epithelium by Wild-Type Stem Cells

(A) ISH for *Olfm4* shows complete loss of stem cells on day 1 with foci of new stem cells on day 3 and reconstitution of stem cells in all crypts by day 5 p.i.

(B) IHC for Grp78 shows loss of Grp78 on day 1, foci of Grp78-positive cells on day 3, and extensively Grp78-positive epithelium by day 5 p.i.

(C) ISH for *Olfm4* and IHC for Grp78 on consecutive slides on day 3 p.i. shows that *Olfm4*+-repopulating stem cells are derived from Grp78-positive wild-type cells.

Original magnifications: (A) and (B) 125×; (C) 200×.

To further examine the possibility that Grp78 mutant stem cells are lost by differentiation, we performed lineage tracing of Grp78 mutant intestinal stem cells. To that end, we crossed *Lgr5-eGFP-ires-CreERT2* mice (Barker et al., 2007) (in short *Lgr5-CreERT2*) into mice with the *Rosa26*^{LacZ} reporter allele. In these mice, *Lgr5*-positive stem cells are marked by expression of eGFP. Expression of eGFP is mosaic with approximately half the crypts containing eGFP-positive stem cells and other crypts being negative. A single injection of tamoxifen induces recombination in a proportion of eGFP-positive stem cells (Barker et al., 2007). Recombination in these cells marks both stem cells and their descendants by expression of LacZ. Thus, both recombined and nonrecombined stem cells could be observed (Figure S3C). By crossing the *Grp78*^{fl} allele into these mice, we could directly monitor the influence of ER stress on the fate of Lgr5-positive stem cells.

In control mice (*Lgr5-CreERT2-Rosa26*^{LacZ}*-Grp78*$^{+/fl}$), a single injection of tamoxifen 48 hr prior to analysis marked LacZ-positive Lgr5 progeny in a proportion of crypts, mostly reaching up to cell position +4 from the crypt base. In *Lgr5-CreERT2-Rosa26*^{LacZ}*-Grp78*$^{fl/fl}$ mutant mice, LacZ+ cells were positioned higher in the crypt, and crypt bases were mostly free of LacZ+ cells (Figures 5H and 5I). A double stain for BrdU and LacZ showed that LacZ-positive cells maintained their proliferative capacity (Figures 5J and 5K), suggesting that the Grp78 mutant cells shift up in the crypt and adopt a TA cell fate. We used Lgr5-driven eGFP expression as a surrogate for expression of Lgr5. We observed the expected LacZ-eGFP double-staining cells in control mice at 48 hr p.i. Examination of LacZ+ cells in crypts of *Lgr5-CreERT2-Rosa26*^{LacZ}*-Grp78*$^{fl/fl}$ mutant mice showed that these cells were almost entirely negative for eGFP (Figures 5L and 5M). Thus, at 48 hr after injection of tamoxifen, recombined cells have shifted up the crypt, lost Lgr5-driven expression of eGFP, but maintain their proliferative capacity as indicated by their capacity to incorporate BrdU. This is consistent with a stem cell to TA cell conversion. We concluded therefore that induction of ER stress by means of loss of Grp78 expression causes CBC stem cells to lose self-renewal capacity and to exit the stem cell pool. Most of these cells adopt a TA cell fate, differentiate, and migrate up the crypt.

Loss of Stemness Occurs in a PERK-eIF2α-Dependent Manner

To analyze whether ER stress causes loss of stemness through UPR signaling, we generated LS174T colon cancer cell lines harboring stable knockdown against UPR components. We treated cells with thapsigargin or SubAB for and analyzed expression of stem cell markers. No rescue was observed in *LS147shXBP1* or *LS174shATF6* cells (Figure S7). Knockdown of PERK partially rescued loss of expression of stem cell markers *LGR5* and *ASCL2* after induction of ER stress (Figure 6A). While PERK knockdown was efficient (88% ± 11%), stress-induced

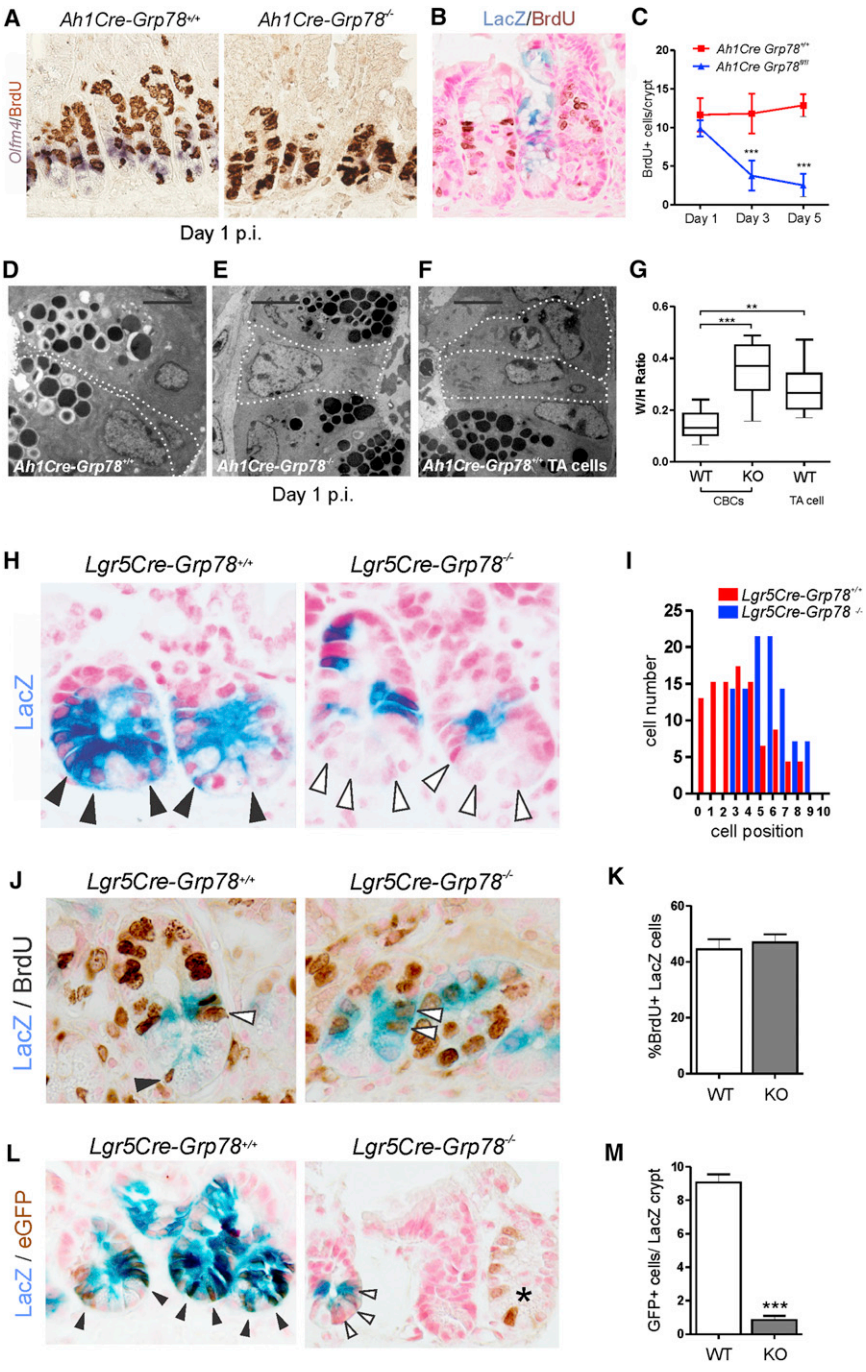

Figure 5. Mutant Stem Cells Are Removed by Differentiation

(A) *Olfm4* ISH and BrdU IHC double staining on day 1 p.i.

(B) Double staining of LacZ and IHC for BrdU shows loss of BrdU-positive cells in remaining Grp78 mutant LacZ-positive crypts at day 5 p.i.

(C) Counting of BrdU-positive cells in recombined crypts ($n \geq 3$/group, >20 crypts counted/animal).

(D) Slender inter-Paneth CBCs on electron micrographs in Grp78 wild-type animals.

(E) In Grp78 mutant mice, CBC cells display an increased width and have adopted the morphological appearance of wild-type TA cells (shown in F). White dashed lines demarcate cell borders.

(F) Transit-amplifying cells in a wild-type mouse have an increased width and content of cytoplasm and organelles compared to wild-type CBCs (shown in D).

(G) Width/height ratio of CBC cells and TA cells in control animals and of CBC cells in *Ah1Cre-Grp78$^{fl/fl}$* mice at day 1 p.i.

(H) LacZ staining on *Lgr5-CreERT2-Rosa26^{LacZ}-Grp78$^{fl/+}$* control mice 2 days after a single injection with 4 mg/kg tamoxifen shows stem cell progeny, marked by LacZ filling the crypts from the CBC cell position upward. In *Lgr5-CreERT2-Rosa26^{LacZ}-Grp78$^{fl/fl}$* mutant mice, LacZ+ cells at the CBC cell position at the crypt base have been lost and progeny is seen in the upper half of the crypt.

(I) Quantification of the distribution of cell positions at day 2 p.i. shows an upward shift of Grp78 mutant cells, away from the crypt base.

(J) Double staining for LacZ and BrdU in wild-type shows both double-positive CBC cells (black arrow head) and TA cells (white arrowhead). In mutant mice, LacZ cells shift up the crypt but remain BrdU positive, indicating a conversion to TA cell phenotype.

(K) Quantification of the percentage of BrdU-positive LacZ cells at day 2 p.i., n = 3 animals per group, >15 crypts counted per genotype.

(L) LacZ and Lgr5^{eGFP} IHC double staining on *Lgr5-CreERT2-Rosa26^{LacZ}-Grp78$^{fl/+}$* control mice at day 2 p.i. shows the expected LacZ and Lgr5^{eGFP} double-positive CBC cells (black arrowheads) giving rise to LacZ+ progeny. In tamoxifen-injected *Lgr5-CreERT2-Rosa26^{LacZ}-Grp78$^{fl/fl}$* mice, LacZ+ (Grp78 mutant) crypts (arrowhead) have lost Lgr5^{eGFP} expression, whereas Lgr5^{eGFP} expression is maintained in a LacZ-negative (nonrecombined, Grp78 wild-type) crypt.

(M) Quantification of the number of eGFP+ cells/LacZ+ crypt at day 2 p.i., n = 3 animals per group, >15 crypts counted per genotype.

Values in (C), (G), (K), and (M) are depicted as mean ± SEM, $^{**}p < 0.01$, $^{***}p < 0.001$. Original magnifications: (A) and (B) 400×; (H), (J), and (L) 800×. See also Figure S6.

phosphorylation of eIF2α was only partially prevented (45% ± 17% reduction in phosphorylation). To obtain complete dephosphorylation of eIF2α, we therefore created a cell line that expressed a constitutively active fragment of GADD34 (GADD34^{ca}), the phosphatase that specifically dephosphorylates eIF2α (Novoa et al., 2001; Oyadomari et al., 2008). This completely rescued loss of stem cell markers in thapsigargin or SubAB-treated LS174T cells (Figure 6A). Interestingly, upon induction of ER stress with SubAB, LS174GADD34^{ca} cells not only rescued stem cell markers, but actually increased

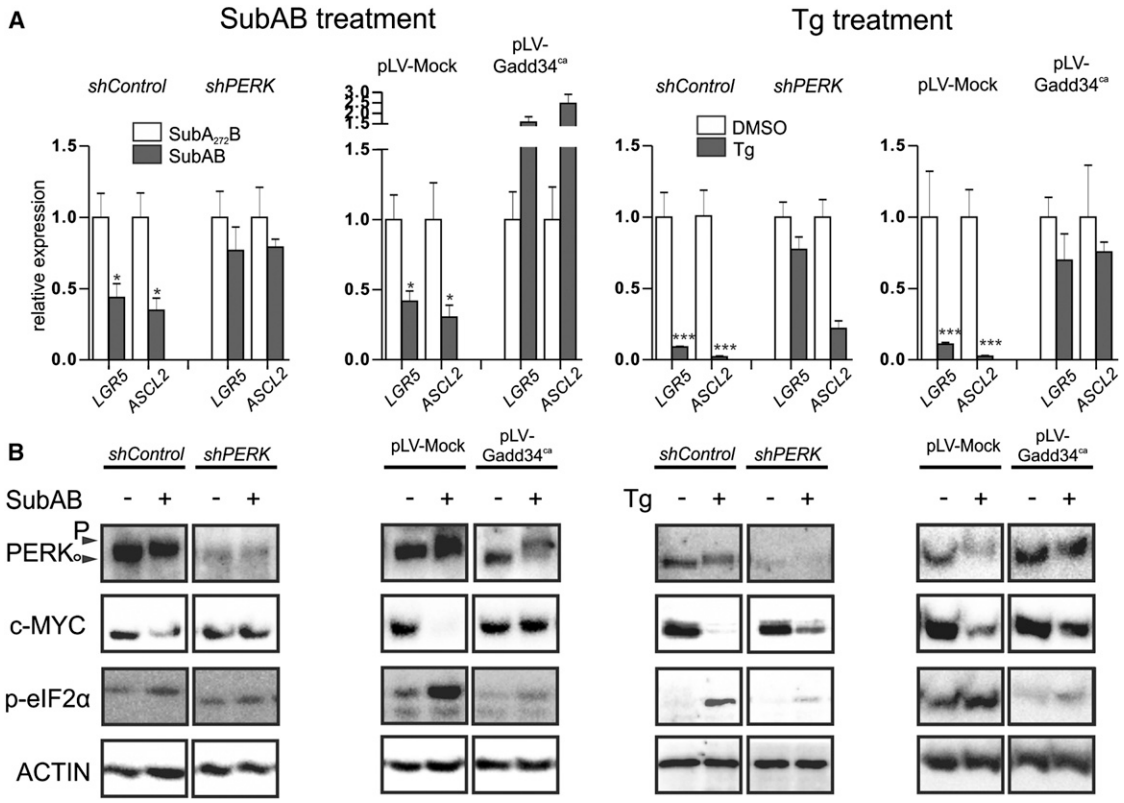

Figure 6. Loss of Stem Cell Markers Occurs in an eIF2α-Dependent Fashion

(A) Quantitative RT-PCR for stem cell markers *LGR5* and *ASCL2* at 24 hr after start of treatment. LS174T were infected with lentiviral constructs as indicated and treated with 100 ng/ml protease dead control $SubA_{A272}B$ versus SubAB or treated with 200 nM thapsigargin versus vehicle.

(B) Immunoblots for c-MYC at 1 hr after the start of treatment. Note that expression of c-MYC protein is inversely correlated with phosphorylation of eIF2α.

Graphs show mean ± SEM, *p < 0.05, ***p < 0.001.

See also Figure S7.

expression of these genes. This may reflect a disturbed balance between the UPR components IRE1α and PERK, which are known to have opposing effects on cell viability (Lin et al., 2009). These data show that ER-stress-induced loss of the stemness signature critically depends on phosphorylation of eIF2α.

Intestinal stem cell fate depends on at least one protein with a very short half-life. c-MYC has a half-life of around 30 min (Hann and Eisenman, 1984), is critical to maintain expression of a core set of Wnt target genes (Sansom et al., 2007), and is known to play a key role in maintenance of intestinal epithelial stem cells (Muncan et al., 2006). To maintain adequate expression levels, proteins such as c-MYC are highly dependent on continuous mRNA translation. Therefore, translation attenuation following eIF2α phosphorylation could affect stem cell fate rapidly and profoundly by blocking translation of these proteins. We performed immunoblots for presence of c-MYC after induction of ER stress and found indeed that within 1 hr protein expression is almost completely lost. In agreement with the rescue of stem cell markers, c-MYC protein translation was rescued partially upon knockdown of PERK. Complete rescue was achieved upon expression of $Gadd34^{ca}$ (Figure 6B). These results suggest that the translation inhibition caused by phosphorylation of eIF2α results in a rapid loss of short-lived proteins with an important role in stem cell fate such as c-MYC.

Perk Signaling Is Required for Stem Cell Differentiation

We next examined whether Perk signaling is not only sufficient for stem cell differentiation, but also required for normal intestinal differentiation. We therefore adapted a recently described method to transduce organoids with murine stem cell virus (Koo et al., 2011) and generated organoids transduced with lentiviral constructs containing small hairpin (shRNA) directed against *Perk* (Figure 7A). To protect cells during infection, organoids were cultured on medium containing the Gsk3β inhibitor CHIR-90221 until 1 week after infection. This hyperactivates Wnt signaling and expands the precursor cell compartment causing a cystic shape of the organoids (Sato et al., 2011). One week after CHIR-90221 withdrawal, we observed that the majority of *shControl* organoids had reverted to a budding shape, which indicates the normal establishment of a differentiated domain of cells at the core of the organoids surrounded by crypt-like structures. In contrast, *shPerk* organoids remained cystic for a longer period (Figures 7A and 7B), suggesting

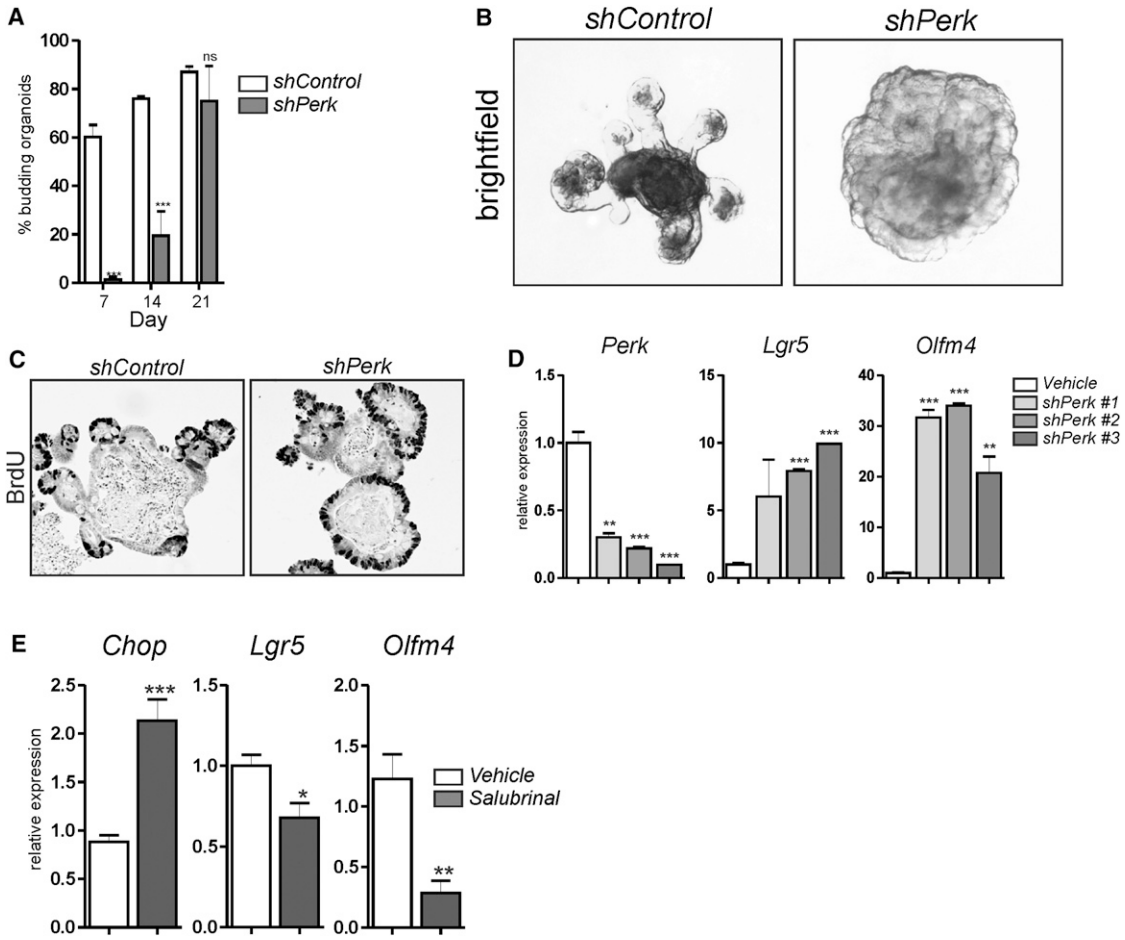

Figure 7. Perk Signaling Regulates Stem Cell Differentiation under Homeostatic Conditions

(A) Quantification of the percentage of budding organoids in at indicated time points (mean of four wells per time point).

(B) Bright-field images of *shControl* and *shPerk* organoids 1 week after withdrawal of CHIR-99021 show the cystic shape of *shPerk* organoids.

(C) BrdU incorporation in *shControl* and *shPerk* organoids.

(D) Quantitative RT-PCR for *Perk*, *Lgr5*, and *Olfm4* in *shPerk*-transduced organoids.

(E) Quantitative RT-PCR for *Chop*, *Lgr5*, and *Olfm4* in organoids treated with 25 μM salubrinal for 24 hr.

Graphs show mean ± SEM, *p < 0.05, **p < 0.01, ***p < 0.001.

a less differentiated phenotype of organoids that lack *Perk*. Three weeks after CHIR-90221 withdrawal, cystic organoids were rare in both groups and shape was stable. Morphologically, *shPerk* organoids consisted of more and larger crypts, budding was more frequent, and the proliferative compartment in crypts was larger (Figure 7C). Transduction with three distinct shRNAs against Perk resulted in downregulation of Perk expression and upregulation of stem cell markers *Lgr5* and *Olfm4* (Figure 7D). Thus, under homeostatic conditions, Perk-eIF2α signaling facilitates stem cell differentiation. We therefore tested whether preventing eIF2α dephosphorylation with the small molecule salubrinal (Boyce et al., 2005) affected the expression of stem cell markers. Treatment with 25 μM salubrinal for 24 hr resulted in increased expression of the Perk-eIF2α target *Chop* and reduced expression of stem cell markers *Lgr5* and *Olfm4*. We conclude not only that ER stress is sufficient for stem cell differentiation, but that physiological ER stress signaling plays a role in differentiation of stem cells under homeostatic conditions.

DISCUSSION

Our data reveal that levels of ER stress and activation of the UPR are low in stem cells compared to TA cells. Activation of Perk-eIF2α signaling is both sufficient and necessary for intestinal epithelial stem cell differentiation.

ER stress and activation of the UPR are associated with differentiation (Iwakoshi et al., 2003; Lee et al., 2005; Wu and Kaufman, 2006), and differentiation of several secretory cell types has been shown to rely on an intact UPR (Kaser et al., 2008; Lee et al., 2005). The possibility that signaling by the UPR may not only be the result of cellular differentiation, but itself be a driving force in cell fate decisions has received little attention. The differential expression of markers of ER stress and

components of the UPR between stem cells and TA cells in the intestinal epithelium suggests that in the intestinal epithelium ER stress may, in fact, mediate a very early and critical step in differentiation, i.e., loss of the capacity for self-renewal. Multiple independent lines of evidence support our conclusion that ER stress is sufficient for intestinal stem cell differentiation. (1) Induction of ER stress results in loss of the stem cell signature in vitro in colon cancer cells and organoids. (2) Deletion of Grp78 results in loss of self-renewal capacity in vivo as was demonstrated by the rapid repopulation of Grp78 mutant epithelium by wild-type cells. (3) Stressed stem cells adopt a TA-cell-like phenotype, characterized by increased cell size and organelle content, while having lost expression of stem cell marker *Olfm4*. (4) Linage tracing demonstrated that Grp78 mutant stem cells lose Lgr5 promoter activity and migrate up the crypt while remaining BrdU positive consistent with a stem cell to TA cell conversion. The accumulation of stem cells in Perk-deficient organoids supports the notion that ER stress is not only sufficient but also necessary for normal stem cell differentiation.

Our finding that Lgr5-positive stem cells are exquisitely sensitive to ER stress is reminiscent of the sensitivity of these cells to gamma irradiation (Yan et al., 2012). Potentially, this indicates converging mechanisms by which stem cells respond to environmental stressors.

We observed a remarkable rate of repopulation with wild-type cells after recombination of *Grp78* with the Ah1Cre. Based on the high efficiency of stem cell recombination in the Ah1Cre that has previously been described, the almost complete loss of stem cells that we observe at 24 hr after recombination, and the absence of extensive crypt fissioning during the repopulation process, we feel that this may have to be explained by alternative mechanisms different from incomplete stem cell recombination. In this light, it is interesting to note that it has recently been demonstrated that *Dll1*-positive partially committed progenitors of the secretory lineage can dedifferentiate and reacquire stem cell characteristics in situations of damage and repair (van Es et al., 2012). Alternatively, it has recently been suggested that a population of cells that is positive for Paneth cell markers may behave as a quiescent stem cell population (Roth et al., 2012). Since the Ah1Cre does not recombine Paneth cells, such cells could be responsible for repopulation in our model.

In conclusion, our data show that there is differential activity of ER stress between stem cells and TA cells in the intestinal epithelium and suggest that the ER may be an important early regulator of intestinal epithelial stem cell differentiation.

EXPERIMENTAL PROCEDURES

Animal Experiments

All animals were housed in the Leiden University Medical Center experimental animal center or in the Academic Medical Center Animal Research Institute and were handled in accordance with guidelines of the local experimental committee. The *Grp78*$^{fl/fl}$ allele (Luo et al., 2006), the *Rosa26*^{LacZ} allele (Soriano, 1999), the *Ah1Cre* allele (Ireland et al., 2004), the *Rosa26*^{ZsGreen} allele (Madisen et al., 2010), and the *Lgr5-eGFP-ires-CreERT2* allele (Barker et al., 2007) have been described previously. In *Ah1Cre*-mice, Cre was induced by intraperitoneal injections with β-naptoflavone in corn oil (80 mg/kg) three times in 12 hr. In *Lgr5-eGFP-ires-CreERT2* mice, Cre was induced by a single intraperitoneal injection with tamoxifen (4 mg/mouse).

Immunohistochemistry, TUNEL Staining, In Situ Hybridization, and X-Gal Staining

The small intestine was divided into three equal parts, proximal, middle, and distal. The analysis described in this report was performed on the middle intestine. For many of the observations made, we sampled both proximal and distal intestine to confirm observations made in the middle intestine and did not find any major differences (data not shown). Tissue was fixed overnight in 10% formalin, embedded in paraffin, and sectioned. For immunohistochemistry, sections were deparaffinized using xylene and rehydrated in a series of ethanols. Endogenous peroxidases were blocked using methanol with 0.3% H_2O_2. For antigen retrieval, tissue was cooked in 0.01 M sodium citrate solution (pH 6.0) for 20 min or, alternatively, in 0.1 M sodium EDTA (pH 9.0) for 20 min. For Xbp1 IHC, slides were additionally blocked for 30 min in TENG-T (10 mM Tris, 5 mM EDTA, 0.15 mM NaCl, 0.25% gelatin, 0.05% Tween 20 [pH 8.0]). Subsequently, slides were incubated with a primary antibody in PBS with 1% bovine serum albumin (BSA) and 0.1% Triton X-100. Sections were then washed and incubated with a PowerVision secondary antibody (Immunologic) for 1 hr. Slides were washed in PBS. Chromagen substrate consisted of diaminobenzidine (Sigma), according to the manufacturer's instructions. For immunohistochemistry, the following antibodies were used: anti-Xbp1 (SC 7160, Santa Cruz), anti-Grp78 (3177, Cell Signaling), anti-phospho-eIF2α (3597, Cell Signaling), anti-BrdU (BMC 9318, Roche), anti-lysozyme (A0099, Dako), and anti-Ascl2 (MAB4418, Millipore).

For TUNEL staining, we used the in situ cell death detection kit from Roche (reference number: 11 684 817 910) according to the manufacturer's instructions.

For in situ hybridization, DNA templates of in situ probes were made by amplification the mRNA of interest. Amplicons were cloned into T-Easy Vector (Promega), according to instructions. Subsequently, dig-labeled probes were made using dig-labeled dUTP (Roche) and transcribed with T7 or Sp6 RNA polymerase (Promega) according to manufacturer's instructions. For hybridization, 4 or 8 μm formalin-fixed paraffin-embedded sections were used. Sections were deparaffinized and rehydrated in H_2O, incubated for 10 min in 1 M HCl, digested with Proteinase K for 20 min, refixed in 4% paraformaldehyde for 10 min, and acetylated with acetic anhydride. Slides were then prehybridized for an hour in a mix of 2% Blocking Powder (Roche), 0.05% Chaps, 50% formamide, 5× saline sodium citrate (SSC) (pH 4.5), 5 mM EDTA, 100 μg/ml heparin (Sigma), and 100 μg/ml yeast RNA (Ambion). Subsequently, slides were incubated for 72 hr at 68°C with a dig-labeled antisense complementary RNA (cRNA) probe. After incubation, slides were washed three times for 20 min at 65°C in a stringency wash buffer containing 50% formamide and 2× SSC (pH 4.5). Slides were then rinsed in TBS with 0.1% Tween 20, blocked with 0.5% Blocking Powder (Roche) in TBS-T, and incubated overnight with sheep anti-dig alkaline-phosphatase-conjugated Fab fragments (Roche). Staining was developed with NBT/BCIP substrate (Sigma) over several hours to several nights.

X-Gal staining was performed by fixing freshly isolated tissues for 90 min at 4°C in PBS containing 1% formaldehyde, 0.2% glutaraldehyde, and 0.02% NP-40. Tissue was washed in ice-cold PBS subsequently and stained overnight in the dark using PBS containing 5 mM $K_3Fe(CN)_6$, 5 mM $K_4Fe(CN)_6$, 2 mM $MgCl_2$, 1 mg/ml X-Gal, and 0.02% NP-40.

Isolation of Lgr5-eGFP+ Cells by Fluorescence-Activated Cell Sorting

Preparation of intestines and subsequent isolation of different populations of eGFP-positive cells based on the level of eGFP expression by fluorescence-activated cell sorting were performed as described previously (van der Flier et al., 2009).

Electron Microscopy and Morphometric Analysis

Pieces of intestine (1 mm^3) were fixed in 1.5% glutaraldehyde in 0.1 M cacodylate buffer at 4°C temperature for several days to several weeks, postfixed in osmium tetraoxide for 1 hr at 4°C, dehydrated in a graded ethanol series, and embedded in an epoxy resin. Sections (110 nm) were contrasted with uranyl acetate and lead citrate and viewed and imaged with a FEI Tecnai 12 transmission electron microscope, operated at 120 kV, and equipped with an Eagle 4k × 4k camera (FEI, Eindhoven, the Netherlands). For measurement

of crypt base columnar cells, at least four animals per genotype were analyzed. Per animal, pictures of two to ten crypts were measured. Crypt base columnar cells were identified by morphological appearance and localization between Paneth cells. For the width measurement, the midnuclear length was taken and divided by the straight distance from the basolateral to the apical side of the cell. Measurements were performed using Image-J version 1.43U (NIH).

Cell-Culture Experiments and Lentiviral Transductions

Cells were grown in Dulbecco's modified Eagle's medium (DMEM) with 10% fetal calf serum (FCS) and 1% penicillin/streptomycin. Lentiviral shRNA contstructs were obtained from the Mission shRNA library (Sigma). The pLV-ca-GADD34 construct was made by subcloning the GADD34 fragment into the pLV vector. Virus was produced according to the manufacturer's instructions. Cells were plated in 1 cm^2 wells until 25% confluency (approximately 10^5 cells per well) and infected with an multiplicity of infection multiplicity of infection of 5. Subsequently, cells were cultured with 5 μg/ml puromycin (Invitrogen) for a week and expanded for experiments.

Organoid Culture and Transduction

We generated organoids as previously described. Organoids were kept on Egf, Noggin, Rspondin1 (ENR) medium. This medium contains N2, B27 supplements (Invitrogen), n-acetylcysteine, 50 ng/ml Egf (Invitrogen), Noggin-Fc-conditioned medium (20%, equivalent to 200 ng/ml), and Rspo1-Fc-conditioned medium (the Rspo1-Fc-expressing cell line was a kind gift from Dr. Calvin Kuo, Stanford). Noggin-Fc-conditioned medium was generated by cloning the murine *Noggin* cDNA into the pFuse plasmid containing the human IgG1 fragment (InvivoGen) to obtain a Noggin-Fc expression vector. Next, 150 cm^2 flasks containing Hek293T cells were transiently transfected with 45 μg Noggin-Fc plasmid per flask, using polyethyleneimine (PEI, Brunswick Scientific) in DMEM medium containing 10% FCS. The next day, medium was changed to DMEM advanced medium without FCS and left for 7 days after which supernatant was harvested. This Noggin-Fc-conditioned medium contains an equivalent of 1 μg/ml of Noggin-Fc.

For lentiviral transductions, we adapted previously described methodology (Koo et al., 2011). Organoids were split to obtain approximately 50 organoids in 20 μl matrigel covered with ENR medium, supplemented with 10 mM nicotinamide (Sigma) and 10 μM CHIR-99021 (Axon Medchem) to generate cystic hyperproliferative organoids. Two days later, hyperproliferative organoids were harvested, disrupted with a Pasteur pipet, and spun down to remove supernatant and matrigel fragments. Next, crypts were trypsinized for 3 min to generate a single cell suspension to which we added high-titer lentivirus in ENR containing nicotinamide, CHIR-99021, 10 μM ROCK inhibitor Y27632 (Sigma), and 8 μg/ml polybrene (Sigma). Cells were transduced, using 1 hr spinoculation at 600 relative centrifugal force at 32°C. Transduced cells were incubated under normal culturing circumstances to recover for 4 hr, resuspended in matrigel, and covered with ENR medium containing nicotinamide, CHIR-90221, and Y-27632. After 3 days, transduced cells were selected using puromycin (4 μg/ml) in ENR medium containing nicotinamide, CHIR-90221, and Y-27632 for 7 days. Surviving cells were further grown on ENR medium without additives.

Immunoblotting

Cells were lysed in cell lysis buffer (Cell Signaling Technology, Leiden, Netherlands) and boiled in sample buffer containing 0.25 M Tris-HCl (pH 6.8), 8% SDS, 30% glycerol, 0.02% bromophenol blue, and 1% β-mercaptoethanol. Separation was done on 10% SDS-PAGE, and proteins were transferred to a polyvinylidene fluoride membrane. Specific detection was done by incubating the blot overnight in TBS with 0.1% Tween 20 with 1% BSA. Antibody binding was visualized using the Lumi-Light western blotting substrate (Roche). For primary detection, the same antibodies were used as for immunohistochemistry with addition of the following antibodies: anti-Actin (SC1616R, Santa Cruz), anti-Perk (5683, Cell Signaling), anti-eIF2α (2106, Cell Signaling), and anti-Chop (2895, Cell Signaling).

RNA Extraction and Quantitative RT-PCR

Cells or tissue was lysed in 1 ml trizol. Tissue was homogenized and RNA extraction was performed according to manufacturer's instructions. For organoid RNA preparations, cells in matrigel were resuspended in 350 μl RLT buffer (RNeasy, QIAGEN) and stored for later use; RNA extraction was performed according to manufacturer's instructions. For cDNA synthesis, 1 μg of RNA was transcribed using Revertaid (Fermentas). Quantitative RT-PCR was performed using SybrGreen (QIAGEN) according to manufacturers' protocol on a BioRad iCycler using specific primers for the mRNA of interest (available upon request).

RNA Microarray Experiments

Cells were harvested in Trizol. RNA was extracted according to the manufacturer's protocol. RNA cleanup was performed using RNeasy kit (QIAGEN). For microarray analysis, RNA was labeled using cRNA labeling kit for Illumina arrays (Ambion) and hybridized with Illumina HT12 Arrays. Differentially expressed genes were extracted using ANOVA test ($p < 0.05$) and FDR post-analysis correction. GSEA were done using GSEA software (Broad Institute of MIT and Harvard). The gene set used is the full list of genes published as Table S1 from the original article describing *Lgr5-eGFP-ires-CreERT2*-sorted cells (van der Flier et al., 2009). Heatmaps were generated using TreeView software generated by the Eisen lab (Stanford).

Statistics

All data are presented as mean ± SEM. Cell-culture experiments were repeated at least three independent times. Statistical analysis of cell-culture experiments was performed by 2-way ANOVA analysis. For animal experiments, Student's t test, 1-way ANOVA tests, or 2-way ANOVA tests were used. All ANOVA tests were followed by Bonferroni's post hoc test for multiple comparisons.

ACCESSION NUMBERS

Microarray data have been deposited in the Gene Expression Omnibus Database with the accession number GSE28466.

SUPPLEMENTAL INFORMATION

Supplemental Information includes seven figures and can be found with this article online at http://dx.doi.org/10.1016/j.celrep.2013.02.031.

LICENSING INFORMATION

ACKNOWLEDGMENTS

The research leading to these results has received funding from the European Research Council under the European Community's Seventh Framework Program (FP7/2007-2013)/European Research Council grant agreement number 241344 (GvdB) and a VIDI grant from the Netherlands Organization for Scientific Research (GvdB).

Received: August 25, 2012
Revised: January 31, 2013
Accepted: February 28, 2013
Published: March 28, 2013

REFERENCES

Barker, N., van Es, J.H., Kuipers, J., Kujala, P., van den Born, M., Cozijnsen, M., Haegebarth, A., Korving, J., Begthel, H., Peters, P.J., and Clevers, H. (2007). Identification of stem cells in small intestine and colon by marker gene Lgr5. Nature *449*, 1003–1007.

Bertolotti, A., Zhang, Y., Hendershot, L.M., Harding, H.P., and Ron, D. (2000). Dynamic interaction of BiP and ER stress transducers in the unfolded-protein response. Nat. Cell Biol. *2*, 326–332.

Boyce, M., Bryant, K.F., Jousse, C., Long, K., Harding, H.P., Scheuner, D., Kaufman, R.J., Ma, D., Coen, D.M., Ron, D., and Yuan, J. (2005). A selective inhibitor of eIF2alpha dephosphorylation protects cells from ER stress. Science *307*, 935–939.

Hann, S.R., and Eisenman, R.N. (1984). Proteins encoded by the human c-myc oncogene: differential expression in neoplastic cells. Mol. Cell. Biol. *4*, 2486–2497.

Harding, H.P., Calfon, M., Urano, F., Novoa, I., and Ron, D. (2002). Transcriptional and translational control in the Mammalian unfolded protein response. Annu. Rev. Cell Dev. Biol. *18*, 575–599.

Ireland, H., Kemp, R., Houghton, C., Howard, L., Clarke, A.R., Sansom, O.J., and Winton, D.J. (2004). Inducible Cre-mediated control of gene expression in the murine gastrointestinal tract: effect of loss of beta-catenin. Gastroenterology *126*, 1236–1246.

Ireland, H., Houghton, C., Howard, L., and Winton, D.J. (2005). Cellular inheritance of a Cre-activated reporter gene to determine Paneth cell longevity in the murine small intestine. Dev. Dyn. *233*, 1332–1336.

Iwakoshi, N.N., Lee, A.H., Vallabhajosyula, P., Otipoby, K.L., Rajewsky, K., and Glimcher, L.H. (2003). Plasma cell differentiation and the unfolded protein response intersect at the transcription factor XBP-1. Nat. Immunol. *4*, 321–329.

Kaser, A., Lee, A.H., Franke, A., Glickman, J.N., Zeissig, S., Tilg, H., Nieuwenhuis, E.E., Higgins, D.E., Schreiber, S., Glimcher, L.H., and Blumberg, R.S. (2008). XBP1 links ER stress to intestinal inflammation and confers genetic risk for human inflammatory bowel disease. Cell *134*, 743–756.

Koo, B.K., Stange, D.E., Sato, T., Karthaus, W., Farin, H.F., Huch, M., van Es, J.H., and Clevers, H. (2011). Controlled gene expression in primary Lgr5 organoid cultures. Nat. Methods *9*, 81–83.

Lee, A.H., Chu, G.C., Iwakoshi, N.N., and Glimcher, L.H. (2005). XBP-1 is required for biogenesis of cellular secretory machinery of exocrine glands. EMBO J. *24*, 4368–4380.

Lin, J.H., Li, H., Zhang, Y., Ron, D., and Walter, P. (2009). Divergent effects of PERK and IRE1 signaling on cell viability. PLoS ONE *4*, e4170.

Luo, S., Mao, C., Lee, B., and Lee, A.S. (2006). GRP78/BiP is required for cell proliferation and protecting the inner cell mass from apoptosis during early mouse embryonic development. Mol. Cell. Biol. *26*, 5688–5697.

Madisen, L., Zwingman, T.A., Sunkin, S.M., Oh, S.W., Zariwala, H.A., Gu, H., Ng, L.L., Palmiter, R.D., Hawrylycz, M.J., Jones, A.R., et al. (2010). A robust and high-throughput Cre reporting and characterization system for the whole mouse brain. Nat. Neurosci. *13*, 133–140.

Mao, C., Dong, D., Little, E., Luo, S., and Lee, A.S. (2004). Transgenic mouse model for monitoring endoplasmic reticulum stress in vivo. Nat. Med. *10*, 1013–1014, author reply 1014.

Muncan, V., Sansom, O.J., Tertoolen, L., Phesse, T.J., Begthel, H., Sancho, E., Cole, A.M., Gregorieff, A., de Alboran, I.M., Clevers, H., and Clarke, A.R. (2006). Rapid loss of intestinal crypts upon conditional deletion of the Wnt/Tcf-4 target gene c-Myc. Mol. Cell. Biol. *26*, 8418–8426.

Muñoz, J., Stange, D.E., Schepers, A.G., van de Wetering, M., Koo, B.K., Itzkovitz, S., Volckmann, R., Kung, K.S., Koster, J., Radulescu, S., et al. (2012). The Lgr5 intestinal stem cell signature: robust expression of proposed quiescent '+4' cell markers. EMBO J. *31*, 3079–3091.

Ni, M., and Lee, A.S. (2007). ER chaperones in mammalian development and human diseases. FEBS Lett. *581*, 3641–3651.

Novoa, I., Zeng, H., Harding, H.P., and Ron, D. (2001). Feedback inhibition of the unfolded protein response by GADD34-mediated dephosphorylation of eIF2alpha. J. Cell Biol. *153*, 1011–1022.

Oyadomari, S., Harding, H.P., Zhang, Y., Oyadomari, M., and Ron, D. (2008). Dephosphorylation of translation initiation factor 2alpha enhances glucose tolerance and attenuates hepatosteatosis in mice. Cell Metab. *7*, 520–532.

Paton, A.W., Beddoe, T., Thorpe, C.M., Whisstock, J.C., Wilce, M.C., Rossjohn, J., Talbot, U.M., and Paton, J.C. (2006). AB5 subtilase cytotoxin inactivates the endoplasmic reticulum chaperone BiP. Nature *443*, 548–552.

Pfaffenbach, K.T., and Lee, A.S. (2011). The critical role of GRP78 in physiologic and pathologic stress. Curr. Opin. Cell Biol. *23*, 150–156.

Roth, S., Franken, P., Sacchetti, A., Kremer, A., Anderson, K., Sansom, O., and Fodde, R. (2012). Paneth cells in intestinal homeostasis and tissue injury. PLoS ONE *7*, e38965.

Sansom, O.J., Meniel, V.S., Muncan, V., Phesse, T.J., Wilkins, J.A., Reed, K.R., Vass, J.K., Athineos, D., Clevers, H., and Clarke, A.R. (2007). Myc deletion rescues Apc deficiency in the small intestine. Nature *446*, 676–679.

Sato, T., Vries, R.G., Snippert, H.J., van de Wetering, M., Barker, N., Stange, D.E., van Es, J.H., Abo, A., Kujala, P., Peters, P.J., and Clevers, H. (2009). Single Lgr5 stem cells build crypt-villus structures in vitro without a mesenchymal niche. Nature *459*, 262–265.

Sato, T., van Es, J.H., Snippert, H.J., Stange, D.E., Vries, R.G., van den Born, M., Barker, N., Shroyer, N.F., van de Wetering, M., and Clevers, H. (2011). Paneth cells constitute the niche for Lgr5 stem cells in intestinal crypts. Nature *469*, 415–418.

Soriano, P. (1999). Generalized lacZ expression with the ROSA26 Cre reporter strain. Nat. Genet. *21*, 70–71.

van de Wetering, M., Sancho, E., Verweij, C., de Lau, W., Oving, I., Hurlstone, A., van der Horn, K., Batlle, E., Coudreuse, D., Haramis, A.P., et al. (2002). The beta-catenin/TCF-4 complex imposes a crypt progenitor phenotype on colorectal cancer cells. Cell *111*, 241–250.

Van der Flier, L.G., Sabates-Bellver, J., Oving, I., Haegebarth, A., De Palo, M., Anti, M., Van Gijn, M.E., Suijkerbuijk, S., Van de Wetering, M., Marra, G., and Clevers, H. (2007). The Intestinal Wnt/TCF Signature. Gastroenterology *132*, 628–632.

van der Flier, L.G., van Gijn, M.E., Hatzis, P., Kujala, P., Haegebarth, A., Stange, D.E., Begthel, H., van den Born, M., Guryev, V., Oving, I., et al. (2009). Transcription factor achaete scute-like 2 controls intestinal stem cell fate. Cell *136*, 903–912.

van Es, J.H., Sato, T., van de Wetering, M., Lyubimova, A., Nee, A.N., Gregorieff, A., Sasaki, N., Zeinstra, L., van den Born, M., Korving, J., et al. (2012). Dll1+ secretory progenitor cells revert to stem cells upon crypt damage. Nat. Cell Biol. *14*, 1099–1104.

Wu, J., and Kaufman, R.J. (2006). From acute ER stress to physiological roles of the Unfolded Protein Response. Cell Death Differ. *13*, 374–384.

Yan, K.S., Chia, L.A., Li, X., Ootani, A., Su, J., Lee, J.Y., Su, N., Luo, Y., Heilshorn, S.C., Amieva, M.R., et al. (2012). The intestinal stem cell markers Bmi1 and Lgr5 identify two functionally distinct populations. Proc. Natl. Acad. Sci. USA *109*, 466–471.